33rd Annual International Conference of the IEEE EMBS
Boston, Massachusetts USA, August 30 - September 3, 2011

Chip-scale Hermetic Feedthroughs for Implantable Bionics

Thomas Guenther, *Student member, IEEE*, Christopher W.D. Dodds *Member, IEEE*,
Nigel H. Lovell, *Fellow, IEEE* and Gregg J. Suaning, *Member, IEEE*

***Abstract*— Most implantable medical devices such as cochlear implants and visual prostheses require protection of the stimulating electronics. This is achieved by way of a hermetic feedthrough system which typically features three important attributes: biocompatibility with the human body, device hermeticity and density of feedthrough conductors. On the quest for building a visual neuroprosthesis, a high number of stimulating channels is required. This has encouraged new technologies with higher rates of production yield and further miniaturization. An Al_2O_3 based feedthrough system has been developed comprising up to 20 platinum feedthroughs per square millimeter. Ceramics substrates are shown to have leak rates below 1×10^{-12} atm×cc/s, thus exceeding the resolution limits of most commercially available leak detectors. A sheet resistance of 0.05 Ω can be achieved. This paper describes the design, fabrication process and hermeticity testing of high density feedthroughs for use in neuroprosthetic implants.**

I. Introduction

Today's implant manufacturers have to address several challenges simultaneously: materials used have to be biocompatible, thus materials are not only limited by processibility. The devices need to remain hermetic over several decades, especially when focusing on retinal implants where multiple surgeries should be avoided. The size of the device needs to be as small as possible to fit into the site of implantation. The size reduction in return lowers the number of water molecules which are allowed to leak into the package until the dew point is reached.

Water leakage into sealed packages cannot be avoided [1]. One can say that it is only a matter of time until enough water molecules have leaked into a package before the dew point is reached. While the water molecules in air are not of concern themselves, the concentration of water molecules cause a problem. If the critical concentration is exceeded, water condenses inside the package which, in the presence of appropriate ions, can lead to short-circuiting of the internal electronics or corrosion and subsequent open circuits. Other failure modes include, but are not limited to, swelling of employed polymers leading to a build-up of pressure of the package, blisters and cracking of bulk material. Derived from the Clausius-Clapeyron relation, the Antoine Equation states that the allowed concentration of molecules at a specific temperature can be calculated specifying when condensation occurs. For example, at body temperature (37 °C) the allowed concentration is approximately 61,000 ppm. Another definition of the dew point being reached is if more than three monolayers of water molecules have accumulated at the internal surfaces of the device. Since the size reduction of the packages down to chip-scale reduces the volume below the range of μL, the total amount of water molecules allowed is very limited. Considering the life-time of an implant, leak rates in the range of 1×10^{-11} atm×cc/s - 1×10^{-10} atm×cc/s need to be achieved. Despite the strong relationship between size and allowed leak rate, absolute values also depend on the internal architecture of the devices. For example the use of 'water-getter' materials would significantly alter the dew point.

Neural stimulators are typically more effective if they employ more stimulation channels. This requirement becomes even more technically difficult as the miniaturization itself raises the need for higher density feedthroughs. Taking a closer look at visual prostheses the advantage of higher channels becomes obvious. The pixelized vision by stimulating the spatiotopically arranged ganglion cells of the retina increases in resolution if more stimulation sites are used, provided each site can produce a unique percept. Thus the need for a large number of feedthroughs is created.

Current literature shows that there are several approaches of bionic vision prosthesis systems around the world, all of them have to deal with similar problems [2]: the available space at the implantation site is limited and the materials must withstand the harsh environment of the human body. Polymeric approaches using modern microtechnologies generally have difficulties with corrosion or delamination of the thin films applied. Except for a few specialized materials, polymers are not hermetic at all. Their capability of acting as a barrier results from their ability to stop the diffusion of ions, thus only deionized water, which does not cause corrosion or short circuits, can make contact with the internal electronics. However, creep leakage of water along the electrode tracks commonly occurs. The necessity of having an opening in the polymeric encapsulation to have an electrode-tissue interface exposes an interface of electrode-encapsulation. Along this interface, water can leak either straight into the package, or it may cause problems at the interconnection of the electrode to the feedthrough in cases where dissimilar materials are used. Dissimilar materials in the presence of electrolytic fluids form a galvanic cell - corrosion and eventual failure of the device is inevitable when this occurs [3].

Manuscript received April 15, 2011. This research was supported by the Australian Research Council (ARC) through its Special Research Initiative (SRI) in Bionic Vision Science and Technology grant to Bionic Vision Australia (BVA) and an ARCs Linkages Project program in collaboration with Cochlear Limited.

T. Guenther, C.W.D. Dodds, N.H. Lovell and G.J. Suaning are with the Faculty of Engineering, Graduate School of Biomedical Engineering, The University of New South Wales, Kensington, NSW, 2052, Australia. Thomas.guenther@unsw.edu.au

Hybrid packages made of ceramics, on the other hand, can handle the problem of the biological environment well. The disadvantage of these so-called hard shell packages is that they are by nature large [4], when giving consideration to the feature sizes which can be achieved using classical thick film technology. Nonetheless, hard shell packages and hybrid packaging have a well-recorded history and are still being employed in some of the successful neural stimulators in clinical use today.

During the last decade, multiple micro-machining technologies have become available and affordable. Combining these modern technologies for miniaturization with the extensively trialled, biocompatible and hermetic properties of hard shell packages, we were able to create high-density, hermetic feedthroughs for implantable bionics made of alumina-based ceramic and platinum (Pt) only. In combination with brazing technologies to join titanium lids, chip-scale packages could be produced. In the following, the methods to create such ceramic substrates are described and analyzed.

II. Methods

A. Design of Hermetic Feedthroughs

Creating feedthroughs requires dealing with the general fact that thermal expansion coefficients of dissimilar materials do not match. Thus cracks at the interface between the materials are common because the internal stresses exceed the bonding force. In a former publication we demonstrated that horizontal tracks in bulk alumina can produce hermetic feedthroughs [5]. Further need for miniaturization has led us to the approach of multilayered ceramics in interaction with Pt pastes. Combining the idea of horizontal feedthroughs and multilayered substrates, our design employs a kink in the feedthrough (Fig. 1). The kink provide a means through which to apply compressive forces before or during sintering to establish a Pt-Al_2O_3 bond as described by Allen and Borbidge [6].

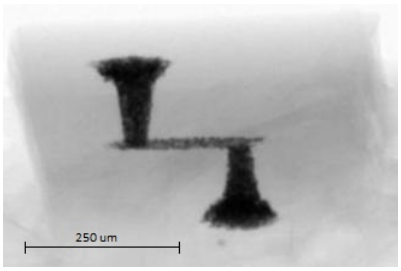

Fig. 1. NanoCT picture of a Pt two layer feedthrough in an Al_2O_3 ceramic with a horizontal, hermetic bridge.

The vertical section of the feedthrough is achieved by penetrating a ceramic layer with a via which is not necessarily required to contribute to the hermetic properties of the feedthrough. From the end of the via a horizontal bridge is created which connects the via of the first layer to the via of the second layer. The method also enables routing of tracks from the output pads of a neurostimulation integrated circuit to the appropriate stimulating electrode. In the following example a four layer structure was shown to connect 98 electrodes and be hermetic.

B. Laser Micro-Machining

An Nd:YAG marking laser (DPL Genesis Marker, ACI) with a scanner head was used as a multi tool for micro-machining. Feature sizes as small as 20 μm can be cut. Computer aided design (CAD) was used to create the designs which were imported into the laser software.

Al_2O_3 particulate, suspended in a wax binder was formed into a tape with a thickness of 200 μm. Laser micro-machined vias were cut and filled with Pt paste consisting of Pt particles and thinners. The Pt paste was printed with a stainless steel stencil and a rubber squeegee across the entire area of the sample. Fig. 2 shows the exploded view of the multilayer structure. In the following the production cycle of each layer is described.

1) Bottom layer: The bottom layer formed the attachment site for laser-patterned Pt micro-electrodes (Fig. 3) [7]. The alumina tape was stuck to a microscope slide to ensure flatness and alignment during processing. Using a hatching function, grooves were laser-cut into a sheet of the alumina tape where tracks were intended later. Subsequently, holes for the vias were cut at the according positions. Pt paste was distributed across the whole surface area. The vias were filled with paste with the aid of pressured air. Finally, the paste was dried in a convection oven to remove all thinners.

2) Middle layers: The middle layers were formed by a method of Pt paste ablation (Fig. 2) [8]. Compared to the bottom layer no grooves were cut. Via holes were cut into the alumina tape and subsequently filled with Pt paste with the aid of pressured air. The paste was dried. A negative image of the designed tracks was created and laser ablated, leaving behind only the supposed tracks.

3) Top layer: The top layer was created in the same way as the bottom layer. Additionally alignment holes were cut into the alumina tape to aid in realignment following inversion of the layered assembly. The bottom of the top layer was coated with Pt paste. Since the sample needed to be removed from its original alignment position it needs to be realigned to the laser to within 5μm. To aid this process, the sample was mounted onto a microscope slide. Custom realignment software was written to compare and align a reference sample with the actual sample using micrographs and adjusting the laser design files accordingly. Subsequently the bottom surface of the top layer was laser-patterned in a similar fashion to the middle layers.

C. Lamination and Sintering

The different alumina sheets were aligned to each other and placed in a uniaxial hot press. Heat and pressure caused the wax in the ceramic tape to melt and consequently the alumina particles at the interfaces of the layers diffuse into each other. The assembly was then placed in a furnace and sintered at a 1500 °C. To ensure flatness, the wax binders of the tapes and the organic vehicles of the Pt paste were burned out carefully. Several dwelling steps were required

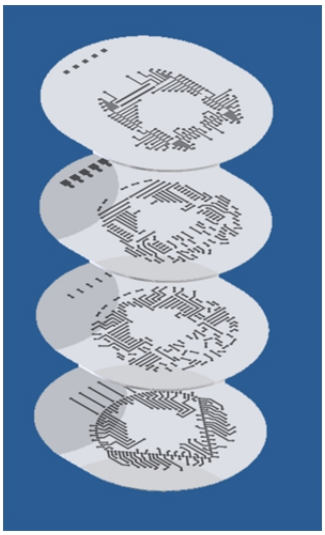

Fig. 2. Exploded view of the four layer substrate showing the routing of the Pt tracks from the chip side to the electrode side.

for a diffusive burn-out without creating gas bubbles which limit the hermeticity by creating leak channels. Additionally, sinter setters were used to reduce friction during sintering while applying slight compression from the weight of the sinter setters.

D. Postprocessing

After sintering the top and bottom layers remained completely covered with Pt paste. Polishing was used to remove all exessive Pt paste and reveal remaining Pt tracks embedded within the bulk alumina. The polished outer surfaces of the alumina were prepared for further processing steps (Fig. 3) [9].

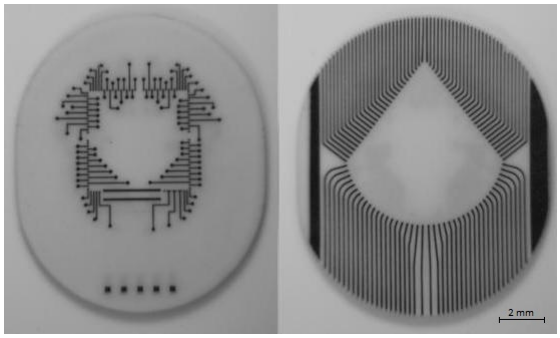

Fig. 3. Left: Top surface of a 98 channel substrate for the attachement of the integrated circuit. Right: Bottom surface of a 98 channel substrate for the attachement of a 98 channel electrode array.

E. Flip-Chip Bonding

As proof of principle, flip-chip bonding of a neurostimulation integrated circuit was tested. Gold (Au) stud bumps were bonded to the chip pads using a wire bonder. The integrated circuit was then flipped onto the ceramic. Thermocompression in combination with ultrasonic energy was used to bond the chip to the ceramic.

F. Hermeticity

Hermeticity tests according to MIL STD 883.1014.A4 were conducted using a helium leak detector. A custom made adapter was designed to hold the ceramic discs on the leak detector. The outside of the ceramic was covered with a helium atmosphere of 1 atm while measurements were taken against a vacuum of 2×10^{-6} atm. A background noise value from helium which leaked into the mass spectrometer was subtracted. In addition, background signals from the surrounding air were subtracted using a dynamic filter function before the helium atmosphere was created. This method allowed a differential measurement of helium leakage through the feedthroughs. Equivalent leak rate limits have been calculated to be 2.8×10^{-11} atm$\times$cc/s assuming a package size of 1 μl and a life-time of 50 years of the implants. Thus, real leak rates measured with the method described above should not exceed 5.6×10^{-11} atm$\times$cc/s.

III. Results

A. Feature Sizes

Feature sizes as small as 20 μm with a pitch distance of 40 μm could be achieved. Film thicknesses had to be kept below 10 μm to avoid an unstable aspect ratio resulting in short-circuiting of the tracks. Feedthough densities of 1000/cm^2 have been achieved.

B. Electrical Properties

Depending on the routing of the Pt tracks, the track length of the horizontal connects can differ widely. Additionally, different designs use different track widths. Thus, the electrical resistance was determined by the sheet resistance of the horizontal bridge, demonstrating thin film characteristics. Tracks have been produced employing the technique used for the top layer and for the middle layers. A sheet resistance of 0.05 Ω could be achieved. The alignment tolerances of less than 50 μm could be maintained and electrical conductivity was ensured. 15 samples with 361 feedthroughs each have been produced. No short circuits could be observed. For simplified measurements of conductivity, one side of the samples was shortcircuited while the feedthroughs could be checked individually from the other side. Electrical conductivity of each single feedthrough was achieved in 15 out of 15 samples with a total of 5415 feedthroughs.

C. Surface and Bulk Properties

The top and the bottom surfaces were measured with a profilometer. 15 lines of 5 mm length on three samples were scanned. Employing the described surface methods resulted in an average surface roughness of 200 nm and an average flatness of 600 nm. In comparison to thin-film techniques, the created devices were not prone to delamination due to the stable Pt-alumina bond created. Cracking due to internal stresses or abrasion due to handling as commonly seen in thin film metallization could not be observed.

Flip-chip bonding was tested on three substrates on its bare Pt surface. Three substrates were electroplated with 24K Au.

While flip-chip bonding on pure Pt was not possible, all three ceramics with electroplated Au were bonded successfully.

D. Hermeticity

Helium leak rates of less than 1×10^{-12} atm×cc/s were recorded for 20 out of 21 samples. One sample showed a gross leak with a leak rate more than 1×10^{-5} atm×cc/s. Precise measurements of the leak rate was limited by the sensitivity of the leak detection system. In addition, leaky substrates were produced to ensure the correct working state of the leak detector and to act as a reference. Reference samples showed leak rates of 1×10^{-9} atm×cc/s and higher.

IV. Discussion and Conclusions

High-density hermetic feedthroughs in hard shell technology using only alumina and Pt could be produced. Combining technologies developed more than 50 years ago with modern micro-machining provides the capability of creating chip-scale hermetic encapsulations. Laser micro-machining in combination with classical screen printing methods has shown an enormous degree of downscaling of the minimum feature sizes. Chip-scale substrates could be produced enabling the use of more advanced bonding techniques than wire bonding. A high yield could be achieved due to the advantage of the multilayer technology which allows process control of the single layers during processing. Only one out of ten substrates showed failure modes not detectable during production. While the resolution of the features formed by the paste is usually defined by the fluidic properties of the pastes and the amount of paste which is printed, the new methods described here are independent of these properties. Nonetheless, the thickness of the Pt paste film needs to be kept to a minimum so that feature sizes of the order of 20 μm with a pitch distance of 40 μm can be achieved. Film thicknesses above 10 μm could create an unstable aspect ratio resulting in short-circuiting of the tracks. The feedthroughs have a sheet resitance of 0.05 Ω, which is negligible in contrast to the kΩ to MΩ impedance of electrode-tissue interfaces.

Studies on firing profiles have shown a very sensitive behavior of paste and ceramic tape due to the outgassing effects of the binders. In general, the firing profile needs to be as slow as possible to create a good bond between the Pt and the alumina, but fast enough to prevent giant grain growth. In addition, other factors require to speed up the process: sample yield and energy costs are the leading reasons. A 30 h sintering profile with multiple dwelling steps in the ramp up cycle could be established resulting in flat, hermetic substrates. Due to the addition of magnesium oxide to prevent giant grain growth, biocompatibility studies according to ISO 10993 have been carried out and showed no adverse effects.

Hermeticity measurements of feedthroughs produced with these optimized parameters have shown leak rates below the detection limit of our machine. The method used is controversial because of its limited exposure time until leaks other than through the feedthroughs are detected. However, different leaks show different behavior: leakage through O-rings builds up slowly and reaches, dependent on the material, a stable value. Faulty feedthroughs show an instant increase of the measured leak rate when a helium atmosphere is created on the outside of a sample. Due to the low leak rates, filling of sealed packages with helium as described in MIL STD 883.1014.A1 is not possible. A more advanced approach is to seal the package in helium atmosphere ensuring a complete filling of the package with helium before testing. Such an apparatus is currently under development.

The shrinkage of the ceramics during sintering is a major disadvantage. To compensate for this effect upscaling and distortion analysis of individual designs is required. While the surface requirements for flip-chip bonding of an integrated surface could be met in terms of roughness and flatness, matching a footprint is more complicated. The pad layout of the substrate has to fit the pad layout of our neurostimulation integrated circuit to tolerances of less than 10 μm at each point of attachment. Thus, process tolerant bonding techniques like Au stud bump bonding need to be used to attach an ASIC to the substrate.

Constrained sintering under uniaxial pressure can overcome these shortcomings. Shrinkage can thus be limited to the z axis only while the x and y dimensions remain stable. Additionally, the density of the ceramics can be increased by employment of this approach.

Studies on hot-pressed sintering of ceramics for implantable bionics are currently being carried out.

V. Acknowledgements

The authors wish to thank George Yang, Sergej Kolke and Sunil Patel from the University of New South Wales, and Timo Bernthaler and Thomas Samtleben from the Aalen University for their substantial support.

References

[1] H. Greenhouse, *Hermeticity of Electronic Packages*, Noyes Publications, Park Ridge, NJ; 2000.

[2] T. Guenther, N.H. Lovell and G.J. Suaning, The bionic eye: system approaches - a review, *Expert Rev. Med. Devic.*, to be published.

[3] A. Vanhoestenberghe, N. Donaldson, N.H. Lovell and G.J. Suaning, Hermetic encapsulation of an implantable vision prosthesis - combining implant fabrication philosophies, *Proc. 13th Ann. Conf. IFESS*, 2008, pp 224-226.

[4] L. Bowman and J.D. Meindl, The packaging of implantable integrated sensors, *IEEE Trans. Biomed. Eng.*, vol. BME-33, no. 2, 1986, pp 248-255.

[5] G.J. Suaning, P. Lavoie, J. Forrester, T. Arminatage and N.H. Lovell, Microelectronic retinal prosthesis: III. A new method for fabrication of high-density hermetic feedthroughs, *Proc. 28th IEEE EMBC*, 2006.

[6] R.V. Allen and W.E. Borbidge, Solid state metal-ceramic bonding of platinum to alumina, *J. Mat. Sci.*, vol. 18, 1983.

[7] G.J. Suaning, M. Schuettler, J.S. Ordonez and N.H. Lovell, Fabrication of multi-layer, high-density micro-electrode arrays for neural stimulation and bio-signal recording, *IEEE EMBS 3rd CNE*, 2007.

[8] J. Ordonez, C. Jeschke, T. Guenther, T. Stieglitz and G.J. Suaning, Laser-structuring of thick-film conductors and its application on an optical stimulator, *Proc. 14th Ann. Conf. IFESS*, 2009.

[9] T. Guenther, A. Mintri, L.H. Jung, T. Lehmann, N.H. Lovell and G.J. Suaning, Laser-micromachined, chip-scaled ceramic carriers for implantable neurostimulators *Proc. 33rd IEEE EMBC*, 2011, submitted.